

Oil Spill Detection by SAR Images Based on Shape Feature Space

Guo Yue¹ and Wang XiaoFeng²

¹Merchant Marine Academy, Shanghai Maritime University, Shanghai, P.R. of China

²Information Engineering College, Shanghai Maritime University, Shanghai, P.R. of China

¹ yueguo@shmtu.edu.cn, ² xfwang@cie.shmtu.edu.cn

ABSTRACT—Using SAR to monitor oil spill is a useful method. Due to the performance of oil spill on SAR images, is similar with other oceanic phenomenon, it is difficult to distinguish between oil spill and "looks-like". In this paper presents a detection method of oil spill which based on feature space shape recognition for the characteristics of SAR images. Firstly, we segment image of oil samples to extract two type regions of oil spill and looks-like. Then we analyze this two types of regions by different shapes characters and combination the characters into a new feature space. Finally, learn to recognize oil spill area by Artificial Neural Networks.

Keywords-SAR,Shape feature,ANN,Oil spill

1. Introduction

Among the different types of marine pollution, oil is a major threat to the worldwide seas ecosystems. The source of the oil pollution can be the mainland or directly at sea. Sea-based sources are mainly discharges coming from ships or off-shore platforms.

Satellites equipped with Synthetic Aperture Radar (SAR), can provide information on the presence of oil at sea. The presence of oil film on the sea surface damps the small capillary and short gravity waves and drastically reduces the Bragg scattering and therefore the measured backscattering energy, resulting in darker areas in SAR imagery[1,2,3]. However, dark areas may be also caused by other phenomena, called 'look-alikes', such as organic film, grease ice, wind front areas, areas sheltered by land, rain cells, currents hear, internal waves and up-welling zones. But SAR imagery is still a common medium for detecting oil spills. In some cases, especially when a large number of SAR scenes has to be examined, the image processing and by eye discrimination between oil spills and lookalikes may be a time consuming as well as labor-intensive task [4]. Several important efforts have already been reported so as to develop an automated detection system that would recognize an oil spill through a SAR image without the intervention of the expert.

Several algorithms have been introduced to automatically detect oil spills from SAR images. Detection of oil spills from SAR imagery can be divided into three steps: (1) detection of dark spots (suspicious slicks), (2) extraction of features from the detected dark spots, and (3) classification of the dark spots (oil spills/look-alikes) [5]. These studies [6,7,8,2,9,10,11,12,13,14] aiming at oil-spill detection have been implemented. Most of these studies rely on the detection of dark areas, which have a high probability of being oil spills. Any formation on the image which is darker than the surrounding area has a probability of being an oil spill and needs further examination.

The previous methods detect a dark spot primarily through its intensity feature; i.e., the intensity in a dark spot is usually lower than the intensity in the background. However, two main difficulties occur when using the intensity domain for detection: (1) SAR imagery is highly speckled due to the constructive and destructive interferences of the reflections from surfaces of objects. Intensity values may show considerable variability, even in the neighborhood of a uniform region[15] and (2) the contrast between dark spots and the background

can vary, depending on the local sea, weather state, the type of oil spill, the resolution and incidence angle of the SAR imagery [16]. These difficulties rule out achieving a robust and fast processing approach for dark-spot detection.

In this research work, we filter and segment the original SAR image by a novel multi-level segmentation method. Thus to get the image region of interest and to prepare for detection. Then we analyzed the segmented image with shape features (Markings ratio, Saturation region, Rectangular saturation, Dispersion, Circularity, Narrow degree, Edge density, Prime of shape), and composed the corresponding eigenvector of shape feature vector into the feature space. Finally, applying artificial neural network to learn the feature space of oil film and looks-alike, and classify the test samples in high confidence. The goal of the research reported in this paper is a new method in the field of oil-films recognition. Through experiments, we proved this method can effectively distinct between oil-films and sea especially oil-films and look-alikes. Compared to other methods, this method, has highly feasible, and the recognition rate is relatively high.

2. Data

Our dataset come from 30 high full synthetic aperture radar (SAR) scene images at 100m resolution in GeoTIF Format. The dataset contains several sea states; all images contain several dark objects and have been used previously by different studies. The satellites include ers-1 and ers-2. The location is South China Sea. The data set not only provides information of satellite but also gives other information in a qualitative or quantitative, such as sea conditions, wind, and wind direction. For oil spills, it gives the number of oil spills in each image and confidence of slick.

Example of oil spills and look-alikes which get from multi-level segmentation method can be seen in Fig. 2. The method was applied on the subset of image of 600×600 rather than complete scenes to speed up the process and to test its performance in terms of time requirements and result quality. From the above 30 SAR images, we extracted 829 look-alikes and 222 oil-films.

3. Method

A methodology is divided into 3 steps. Firstly, Preprocessing the SAR image to get a region of interest in SAR images include oil film and look-alike. Secondly, compute 10 shape characteristics of each, and calculated shape features of each samples, then composed all the feature vector into feature space. Finally, using two layer neural networks learning feature vector of oil film and look alike, classify and recognize the test sample. (See Figure.1)

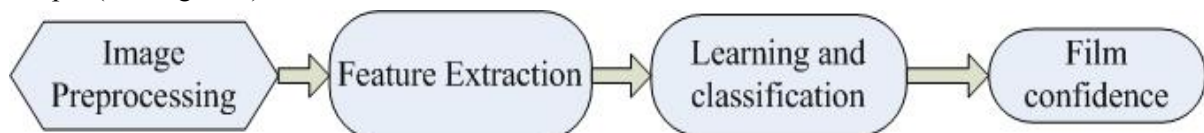


Figure 1 . Overall structure of the method

3.1 Extracting Region of interest

A multi-level methodology to segment the original image this method is divided into 7 steps. We filter the original SAR image by LEE filter, and get the binaries image with Otsu's method. As the binary operation will loss details of oil films inevitably. Therefore, we apply morphological open operations to restore some lost information. After this, there is much spark noise in the images too. So using Lee filter de-noises it again. Since coherence filtering (CF) is an anisotropic non-linear tensor based diffusion algorithm for edge enhancing image filtering. It works well on SAR images segmentation, the noise in the oil films is gone and the edges are connected. While CF will blur the image more or less, we apply Fuzzy C-Means (FCM) to filter the blurring noise. Finally, using dilate operation to restore part of the lost information again. We can compared original image and segmentation results in figure(2).

3.2 Shape feature space

Oil spill area is basically showing irregular region on the sea. Moreover, SAR is gray-scale image no color features. In this work, we analysis of a variety of shape features according to the oil spill images which

obtained from the above method. A brief description was made on common recognize method between oil film and look alike. We select eleven geometric characters to describe the shape feature.[17].

1) *Markings ratio*

Describe the proportion of all the closed areas (spots) in the image .This characters is affine invariant, compute as:

$$\text{Markings ratio} = S / \text{Area} \quad (1)$$

S is the actual number of pixels in each interested region; Area is the total Number of pixels in the image area.

2) *Solidity*

This scalar specifies the proportion of the pixels in the convex hull which in the region. This is also affine features, in fact, reflects the region's solid level of reliability. Computed as

$$\text{Solidity} = \text{Area} / \text{ConvexArea} \quad (2)$$

ConvexArea specifies the number of pixels in convex image

3) *Extent*

This scalar specifies the ratio of pixels in the region to pixels of the total bounding box. This is also affine feature, in fact, reflects the regional expansion of the scope of. Computed as :

$$\text{Extent} = \text{Area} / B_{\text{area}} \quad (3)$$

B_{area} he area of the bounding box.

4) *Dispersion*

Dispersion is commonly used discrete index which represent the complexity of the shape, we use the following formula to calculate the dispersion p:

$$p = S^2 / A \quad (4)$$

where, S is the perimeter, A is the area. The type describes the perimeter per unit area the size of the region. The greater the dispersion, the regional more discrete, and relative to the center of mass.

5) *Circular degree*

Circular degree used to characterize the complexity of the object boundary, for example, compare the same area of the circle and star. The circumference of star is much larger than that of circle. Therefore, we can use circular degrees C to represent the complexity of the shape of the object

$$C = L^2 / A \quad (5)$$

where, L is the region perimeter, A is the size of the area. Analysis shows that when the image area is circle, C has a minimum value 2π . For other shape, $C > 4\pi$. And more complex shapes, C value will greater.

6) *Narrow degree*

Narrow degree, usually refers to the length axis of the inertia ratio. In this paper, definition of normalized.

$$e = 1 - \frac{b}{a} \quad (6)$$

Where a is the object of the long axis, b is the short axis of the object. Degree reflects the narrow level of the shape. For example, a narrow degree of circle is 0; the square is 1. Greater of the narrow degree, more slender of the object.

7) *Edge density*

Edge density refers to that there is step change around the nearby pixel of a set of all the pixels. Edge is discontinuous gray. There generally exists edge between the target and background, goals and objectives. Edge is also an important characteristic of image segmentation. Edge density describes the distribution-information of graphic. Computed as

$$D = P / A \quad (7)$$

where P is the circumference of the area, A is the area.

8) *Prime number of shape(PNS)*

Used to reflect the degree of stenosis of the goals, Computed as

$$PN = A^2 / P^2 \quad (8)$$

where A is the area, P is the circumference of the area.

9) *Interior angles based on bounding rectangle (IABR)*

Interior angles of Polygon is very important on the shape of the expression and recognition, can be expressed as

$$\text{Intra - angle} = \{\alpha_1, \alpha_2, \dots, \alpha_n\} \quad (9)$$

α_i is one of interior angle of the shape. Obviously, the shape description based on interior angles, which has nothing to do with location and shape, rotation and size, So it is very suitable for image retrieval system.

- Vertices: the more the number of polygon vertices, the more complex shape. We consider it is rationally that two shapes with different number of vertices are not similar.
- Angles Mean: Average of all angles of the polygon from the polygon can reflect the shape properties to some extent. For example, the angles mean of a triangle the is 60 degrees, with a big difference between 90 degrees in rectangular.
- Standard deviation of polygon angles

$$\delta = \sqrt{\sum_{i=1}^n (a_i - \bar{a})^2} \quad (10)$$

- Where \bar{a} is the Mean of angles, The standard deviation δ is a general description of the polygon. The polygons is more regular, the value of δ is smaller. Therefore, it can be used to distinguish between regular polygons and irregular polygons.

10) *Hu moment invariant(Hu)*

Hu derived seven moment invariants that are invariant under translation, rotation and scaling of the object[18]. These moment invariants expressions from algebraic invariants applied to the moment generating function under a rotation transformation. They consist of groups of nonlinear centralized moment expressions. The result is a set of absolute orthogonal (i.e. rotation) moment invariants, which can be used for scale, position, and rotation invariant pattern identification. These were used in a simple pattern recognition experiment to successfully identify various typed characters. So utilize it in oil film recognition.

11) *Elliptical Fourier descriptors (EFD)*

EFD representation contains shape information in the low frequency components. EFD is the key for achieving low computational cost while preserving the accuracy of the approximation, as compared to other existing techniques. EFD also implies various algebraic and geometric invariants [19].

Following Yip et al. (1994), let T be an arbitrary positive real number and let $C(t): [0..T] \rightarrow R^2$,

$$C(t) = (x(t), y(t)) \quad (11)$$

is a planar curve parameterized by t, such that $C(t) \in C^{(2)}$. We can describe the curve in Eq. (1) using elliptic Fourier descriptors as follows:

$$\begin{pmatrix} x(t) \\ y(t) \end{pmatrix} = \sum_{t=0}^{\infty} \begin{pmatrix} a_i & b_i \\ c_i & d_i \end{pmatrix} \begin{pmatrix} \cos(\frac{2i\pi t}{T}) \\ \sin(\frac{2i\pi t}{T}) \end{pmatrix} \quad (12)$$

where

$$\begin{aligned} a_0 &= \frac{1}{T} \int_0^T x(t) dt, & b_0 &= 0, & c_0 &= 0, & d_0 &= \frac{1}{T} \int_0^T y(t) dt \\ a_i &= \frac{2}{T} \int_0^T x(t) \cos(\frac{2\pi i t}{T}) dt, & b_i &= \frac{2}{T} \int_0^T x(t) \sin(\frac{2\pi i t}{T}) dt \\ c_i &= \frac{2}{T} \int_0^T y(t) \cos(\frac{2\pi i t}{T}) dt, & d_i &= \frac{2}{T} \int_0^T y(t) \sin(\frac{2\pi i t}{T}) dt \end{aligned}$$

For any $i \in N - \{0\}$. Since $\cos(\cdot)$ and $\sin(\cdot)$ are continuous functions, the inerrability of C(t) ensures existence of the above integrals.

The idea of encoding most of the information in low frequency components is re-iterated in [20], where the authors employ EFD towards learning and modeling shapes that manifest minimal description lengths. Accordingly, contours of objects are decomposed into a series of elliptical harmonics. In another work [21], the authors advocate the use of EFD, among other parametric representations, for segmentation.

Generally, these selected geometric characters can reflect the most features of irregular image. After getting the characteristics of shapes in these oil films and look-alikes, which will form feature matrix for learning and classification.

3.3 Learning and recognition based on ANN

Reference the location of the oil spill marked in the data set. We can remove non-slick in sample which get from pretreatment (ORI), and get the binary image only contain oil spills. We call these binary images as oil spill samples. The samples of non-slick can be getting from:

$$N = Pr \ominus S \quad (13)$$

where Pr is pretreatment images is oil Spill sample. In this work, a self-organization artificial neural net was created .We use a two-layer feed-forward network with sigmoid hidden neurons and linear output neurons can fit multi-dimensional mapping problems arbitrarily well, which given consistent data and enough neurons in its hidden layer.

4. Experiments and Results

We de-noise and segment SAR image by applying a multi-level method [], we extracted the oil spill area from the original SAR image. As the region still include some non-spill (look-alikes), so we confirm location of oil films by the coordinates which given in our dataset. Then getting oil spill area and non-oil spill area respectively by automatic calculation.

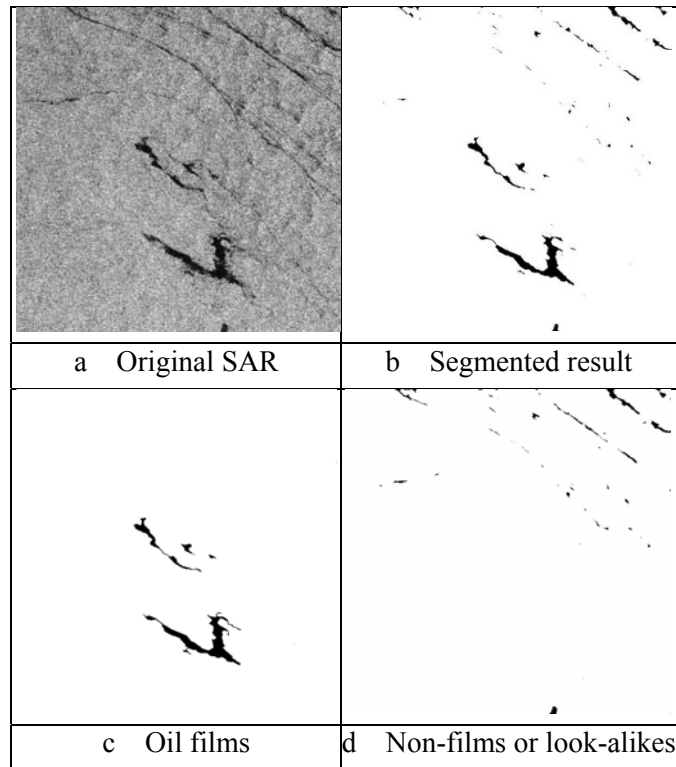


Figure 2 . a) Original SAR image which contains oil-films and look-alikes. b) Image after segmentation and de-noised by multi-level method. c) oil-spill film computed by coordinates of dataset d) Non-spill or look-alikes in the scene.

Thus we get the simples of oil films and non-spills. We applied our approach to all 34 SAR images which contain 222 oil films area and 829 look-alikes films. First, we compare the mean and variance of shape characteristics between oil films and look-alkies.(see table 1)

We get distance between oil-films and used mean and variance of designed a distance formula to visually express the distance between each feature.

$$D_{\text{Mean}} = |M_{\text{Oil}} - M_{\text{Non-oil}}| \quad (14)$$

$$U_{\text{Distance}} = \frac{D_{\text{Mean}}}{\text{Max}(M_{\text{Oil}}, M_{\text{Non-oil}}) - \text{Min}(M_{\text{Oil}}, M_{\text{Non-oil}})} \quad (15)$$

$$D_{\text{Class}} = D_{\text{Mean}} - \text{Max}\{V_{\text{oil}}, V_{\text{Non-oil}}\} \quad (16)$$

M_{oil} and $M_{\text{Non-oil}}$ are mean of oil-film and non-oil or look-alikes feature respectively, V_{oil} and $V_{\text{Non-oil}}$ are variance of oil-film and non-oil or look-alikes feature. D_{Mean} is distance of means. U_{Distance} is the Normalized value of D_{Mean} . The higher the value of U_{Distance} , the more appropriate classification of the feature. D_{Class} shows whether distance between means greater than the biggest variance among oil-films and non-oil. This three data comparison in the following table 1.

TABLE I. Compare Parameters in Different Shapes Characteristics

| Shape Feature | D_{Mean} | U_{Distance} | D_{Class} |
|-----------------|-------------------|-----------------------|--------------------|
| Markings ratio | 0.015 | 0.016 | 0.003 |
| Solidity | 0.174 | 0.192 | 0.1163 |
| Extent | 0.131 | 0.134 | 0.085 |
| Dispersion | 82.74 | 0.094 | -1.981e+04 |
| Circular degree | 6.584 | 0.094 | -119.4 |
| Narrow degree | 0.052 | 0.053 | 0.008 |
| Edge density | 0.468 | 0.210 | 0.309 |
| IABR | 13.85 | 0.154 | -700.1 |
| PNS | 307.3 | 0.014 | -6.578e+06 |
| Hu-1 | 1.201 | 0.018 | -64.74 |
| Hu-2 | 62.36 | 0.014 | -2.111e+05 |
| Hu-3 | 4013 | 0.013 | -9.336e+08 |
| Hu-4 | 4727 | 0.015 | -1.181e+09 |
| Hu-5 | 1.122e+09 | 0.012 | -9.037e+19 |
| Hu-6 | 2.669e+05 | 0.013 | -4.451e+12 |
| Hu-7 | 2.272e+06 | 0.006 | -1.053e+15 |

As can be seen from the Table I, most shape feature mean are close. We chose a relatively large U_{Distance} and D_{Class} value and compared their value by Figure3

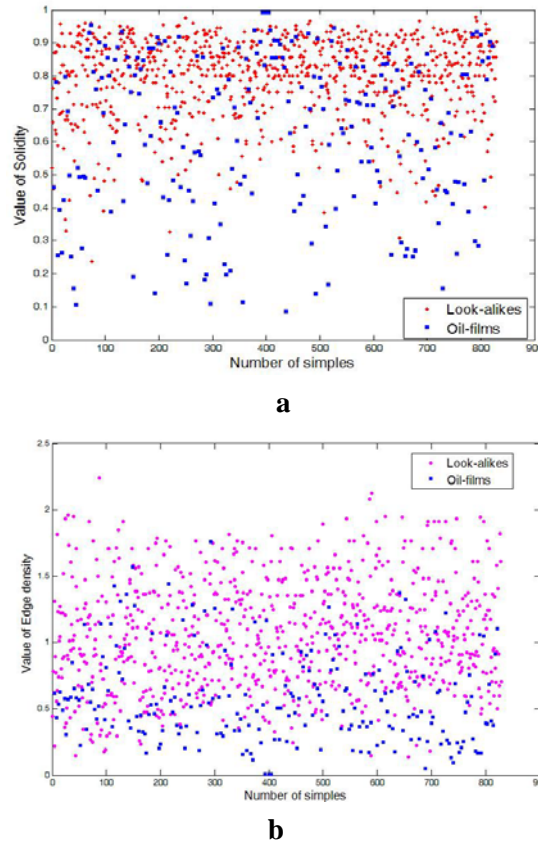


Figure 3 . Choose two feature which U_{Distance} and D_{Class} are bigger than others a) Distribution of Solidity between oil-films and look-alikes b) Distribution of Edge density between oil-films and look-alikes

Therefore, these shape features cannot be directly applied to classify. So we try to apply supervised learning methods to classify these features. First, compose the eigenvalue of sample to matrix. The feature

matrix is divided into two categories, including oil- films and the look-alikes matrix .Oil-films is a 95*222 matrix, which compose of 222 samples For each sample get 95 shape characteristics.

Then, we design a two-layer neural network, hidden layer are 20 neurons. There are 735(70% of all samples) samples use to optimize the network. Accounted for 158 of all samples used to stop training for best generation. And 158 samples used to evaluate network performance. We have two areas to illustrate the results.

1) Performance

It can be seen from the Figure 4 that horizontal axis represents the number of iterations, the vertical axis is error. When ANN iterations reach the 38th, the program reaches the default precision, iteration stops. Iteration stop error is 0.086. This shows that application of this classification, process can converge after little iteration.

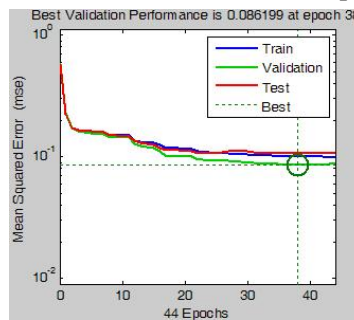


Figure 4 . ANN Classification performance

2) Accuracy

For Figure(5.a),the class 1 is oil-films and class 2 is look-alikes. It can be seen from the confusion matrix, the accuracy classification rate reaches 87.6%. Although the sensitivity is not so high, only at 62.6%., but the positive predicted value and specificity are relatively high, which are 90.4%, and 94.3%, respectively. As figure (5.b) ROC curve farther away from the diagonal line, indicating that these feature has a strong ability to identify subjects.

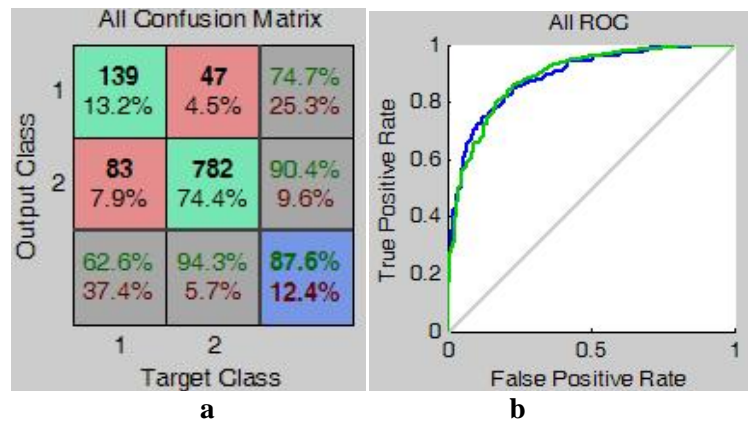


Figure 5 . ANN Classification accuracy a)Confusion matrix of Classification results b) receive operating characteristic curve of Classification results

5. Conclusion — Discussion

This study presents a methodology those identify oil-films from look-alikes in SAR image. The identification task in the proposed methodology acts globally, and is based on geometry shape characteristics learning and classification of features with artificial neural network. Experimental results show that the method can effectively classify the oil-films from SAR image. Through this work we can effectively analyze the positioning of marine oil spill. It provides a good basis for the emergency response to oil spill in the sea.

6. Acknowledgments

This work was developed with partial financial support from key projects of Science and Technology Commission of Shanghai .Project Number is:08240510800.

7. References

- [1] Kubat, M., Holte, R.C., Matwin, S., 1998. Machine learning for the detection of oil spills in satellite radar images. *Machine Learning* 30 (2–3), 195–215.
- [2] Solberg, A., Storvik, G., Solberg, R., Volden, E., 1999. Automatic detection of oil spills in ERS SAR images. *IEEE Transactions on Geoscience and Remote Sensing* 37 (4),1916–1924
- [3] Del Frate, F., Petrocchi, A., Lichtenegger, J., Calabresi, G., 2000. Neural networks for oil spill detection using ERS-SAR data. *IEEE Transactions on Geoscience and Remote Sensing* 38 (5), 2282–2287.
- [4] Gade, M., Redondo, J.M., 1999. Marine pollution in European coastal waters monitored by the ERS-2 SAR: a comprehensive statistical analysis. In: *Proceedings of Geoscience and Remote Sensing Symposium, 1999, IGARSS'99. Hamburg, Germany, 28 June–2 July 1999.* IEEE Geoscience and Remote Sensing Society, USA, vol. 2, pp. 1375–1377
- [5] Brekke, C., Solberg, A., 2005. Feature Extraction for Oil Spill Detection Based on SAR Images. *Lecture notes in computer science*, vol. 3540/2005, pp. 75–84. doi:10.1007/b137285.
- [6] Brekke, C., & Solberg, A. H. S. (2005). Oil spill detection by satellite remote sensing. *Remote Sensing of Environment*, 95(1), 1–13.
- [7] Ziemke, T., 1996. Radar image segmentation using recurrent artificial neural networks. *Pattern Recognition Letters* 17 (4), 319–334.
- [8] Kubat, M., Holte, R.C., Matwin, S., 1998. Machine learning for the detection of oil spills in satellite radar images. *Machine Learning* 30(2–3), 195–215.
- [9] Del Frate, F., Petrocchi, A., Lichtenegger, J., Calabresi, G., 2000. Neural networks for oil spill detection using ERS-SAR data. *IEEE Transactions on Geoscience and Remote Sensing* 38 (5),2282–2287.
- [10] Fiscella, B., Giancaspro, A., Nirchio, F., Pavese, P., Trivero, P., 2000. Oil spill detection using marine SAR images. *International Journal of Remote Sensing* 21 (18), 3561–3566.
- [11] Nirchio, F., Sorgente, M., Giancaspro, A., Biamino, W., Parisato, E., Ravera, R., Trivero, P., 2005. Automatic detection of oil spills from SAR images. *International Journal of Remote Sensing* 26 (6),1157–1174.
- [12] Ferraro, G., Bernardini, A., David, M., Meyer-Roux, S., Muellenhoff, O., Perkovic, M., Tarchi, D., Topouzelis, K., 2007. Towards an operational use of space imagery for oil pollution monitoring in the Mediterranean Basin: a demonstration in the Adriatic Sea. *Marine Pollution Bulletin* 2007 (54), 403–422.
- [13] Ferraro, G., Meyer-Roux, S., Muellenhoff, O., Pavliha, M., Svetak, J., Tarchi, D., Topouzelis, K., 2009. Long term monitoring of oil spills in European Seas. *International Journal of Remote Sensing* 30 (3), 627–645.
- [14] Karathanassi, V., Topouzelis, K., Pavlakis, P., & Rokos, D. (2006). An object-oriented methodology to detect oil spills. *International Journal of Remote Sensing*, 27, 5235–5251.
- [15] Oliver, C., & Quegan, S. (1998). *Understanding synthetic aperture radar images*. London: Artech House.
- [16] Topouzelis, K., Karathanassi, V., Pavlakis, P., & Rokos, D. (2008). Dark formation detection using neural networks. *International Journal of Remote Sensing*, 29, 4705–4720
- [17] Jing AiBing (2009) *Research on Visual Feature Analysis and Classification of Network Education Graphics Resources* Master's degree thesis Shandong Normal University,
- [18] MIAO Jing, YANG Yong, GU Xinchao, *The Moment Invariants and Its Appliance of Image Retrieval Based on Shape Features*, *Journal of Changchun University of Science and Technology (Natural Science Edition)* Vol.32 No.1 Mar.2009
- [19] ZHANG Jin-hua, FU Shan *Shape Recognition Based on Fourier Descriptor of Moments MicroComputer* Vol25 No12-1 2009
- [20] Wang, S., Qi, F., Li, H., 2006. Minimum description length shape model based on elliptic fourier descriptors. In: *Lecture Notes in Computer Science, Advances in Neural Networks – The Third Internat. Symposium on Neural Networks*, vol.3972, pp. 646–651.
- [21] Staib, H.L., Duncan, J., 1992. Boundary finding with parametrically deformable models. *IEEE Trans. Pattern Anal. Machine Intell.* 14 (10), 1061–1075.